

Semi-smooth Newton Algorithm for Non-Convex Penalized Linear Regression

Yueyong Shi^{1,4}, Jian Huang², Yuling Jiao³, and Qinglong Yang³

¹School of Economics and Management, China University of Geosciences, Wuhan,
Hubei 430074, P.R.China

² Department of Applied Mathematics, The Hong Kong Polytechnic University, Hong
Kong 999077, P.R.China

³ School of Statistics and Mathematics, Zhongnan University of Economics and Law,
Wuhan, Hubei 430073, P.R.China

⁴Center for Resources and Environmental Economic Research, China University of
Geosciences, Wuhan, Hubei 430074, P.R.China

Abstract

Both the smoothly clipped absolute deviation (SCAD) and the minimax concave penalty (MCP) penalized linear regression models are capable of dealing with variable selection and parameter estimation simultaneously. Theoretically, these two models enjoy the oracle property even in the high dimensional settings where the number of predictors p may be much larger than the number of observations n . However, numerically, it is quite challenging to develop fast and stable algorithms due to their non-convexity and non-smoothness. In this paper we develop a fast algorithm for SCAD and MCP penalized problems. First, we derive that the global minimizers of both models are roots of some non-smooth equations. Then, Semi-smooth Newton (SSN) algorithm is employed to solve the equations. We prove the local superlinear convergence of SSN algorithm. Computational complexity analysis demonstrates that the cost of SSN algorithm per iteration is $O(np)$. Combining with the warmstarting technique SSN algorithm can be very efficient. Simulation studies and real data examples show that SSN algorithm greatly outperforms coordinate descent in computational efficiency while reaching comparable accuracy.

Keywords: Convergence, MCP, SCAD, Semi-smooth Newton algorithm, Warmstarting

2010 MR Subject Classification 62F12, 62J05, 62J07

1 Introduction

This paper introduces a fast algorithm for concavely penalized regression. We focus on the linear regression model

$$y = X\beta^\dagger + \varepsilon, \quad (1.1)$$

where $y \in \mathbb{R}^n$ is an $n \times 1$ vector of response variables, $X = (X_1, \dots, X_p)$ is an $n \times p$ design matrix, ε is an $n \times 1$ vector of error terms, and $\beta^\dagger = (\beta_1^\dagger, \dots, \beta_p^\dagger)^T \in \mathbb{R}^p$ is the underlying regression coefficient vector.

Under the sparsity assumption that the number of important predictors is relatively small, it is natural to consider the estimator that solves the minimization problem:

$$\min_{\beta \in \mathbb{R}^p} \|X\beta - y\|_2^2, \quad \text{subject to} \quad \|\beta\|_0 \leq \tau, \quad (1.2)$$

where $\|\beta\|_0$ denotes the number of nonzero elements of β and $\tau > 0$ is a tuning parameter controlling the sparsity level. However, the minimization problem (1.2) is NP-hard [Natarajan (1995)], hence it is quite challenging to design a feasible algorithm for solving it when p is large. Replacing the $\|\beta\|_0$ term in (1.2) by $\|\beta\|_1$, we get the ℓ_1 penalized problem or the lasso [Tibshirani (1996)]

$$\min_{\beta \in \mathbb{R}^p} \|X\beta - y\|_2^2, \quad \text{subject to} \quad \|\beta\|_1 \leq \tau. \quad (1.3)$$

which can be viewed as a convex relaxation of (1.2). Numerically, it is convenient to consider the Lagrange form of (1.3):

$$\min_{\beta \in \mathbb{R}^p} \frac{1}{2} \|X\beta - y\|_2^2 + \lambda \|\beta\|_1. \quad (1.4)$$

This is known as "basis pursuit" in the signal processing literature [Chen et al. (2001)]. Computationally, (1.4) is a convex minimization problem, therefore, several fast algorithms have been proposed for computing its global minimizer, such as Homotopy or LARS [Osborne et al. (2000); Efron et al. (2004)] and coordinate descent (CD) algorithm [Fu (1998); Friedman et al. (2007); Wu and Lange (2008)].

Theoretically, under certain regularity conditions on the design matrix X , such as restricted isometry property [Candes and Tao (2005)], strong irrepresentable condition [Meinshausen and Bühlmann (2006); Zhao and Yu (2006)] and sparsity condition on the regression coefficients, lasso has attractive estimation and selection properties. However, even under these conditions, the minimizer of (1.4) still suffers from the so-called lasso bias, which implies that the lasso regularized estimator does not have the oracle property. To remedy this problem, Fan and Li (2001) proposed using concave penalties that can reduce bias and still yield sparse solutions.

This leads to the following minimization problem

$$\min_{\beta \in \mathbb{R}^p} \frac{1}{2} \|X\beta - y\|_2^2 + \sum_{j=1}^p p(\beta_j; \lambda, \gamma), \quad (1.5)$$

where $p(\cdot; \lambda, \gamma)$ is a concave function with penalty parameter λ and γ is a given parameter that controls the concavity of p . We will focus on the smoothly clipped absolute deviation (SCAD) penalty [Fan and Li (2001)] and the minimax concave penalty (MCP) [Zhang (2010a)].

The SCAD penalty is

$$p_{scad}(t; \lambda, \gamma) = \lambda \int_0^t \min\{1, (\gamma - x/\lambda)_+ / (\gamma - 1)\} dx, \gamma > 2, \quad (1.6)$$

and the MCP takes the form

$$p_{mcp}(t; \lambda, \gamma) = \lambda \int_0^t (1 - x/(\gamma\lambda))_+ dx, \gamma > 1, \quad (1.7)$$

where γ is a parameter that controls the concavity of the penalty function and x_+ is the non-negative part of x , i.e., $x_+ = x1_{\{x \geq 0\}}$. In particular, both penalties converge to the ℓ_1 penalty as $\gamma \rightarrow \infty$, and the MCP converges to the hard-thresholding penalty as $\gamma \rightarrow 1$. The MCP can be easily understood by considering its derivative,

$$\dot{p}_{mcp}(t; \lambda, \gamma) = \lambda(1 - |t|/(\gamma\lambda))_+ \text{sign}(t), \quad (1.8)$$

where $\text{sign}(t) = -1, 0$, or 1 if $t < 0, = 0$, or > 0 . The MCP provides a continuum of penalties with the ℓ_1 penalty at $\gamma = \infty$ and the hard-thresholding penalty as $\gamma \rightarrow 1$.

Concavely penalized estimators have the asymptotic oracle property under appropriate conditions [Fan and Li (2001); Zhang (2010a)]. However, it is quite challenging to solve (1.5) with (1.6) and (1.7) numerically, since the objective functions to be minimized are both non-convex and non-smooth. Several methods have been proposed to deal with this difficulty. The first type of methods can be viewed as special cases of MM algorithm [Lange et al. (2000)] or of multi-stage convex relaxation [Zhang (2010b)], such as local quadratic approximation (LQA) of the penalty [Fan and Li (2001)] and local linear approximation (LLA) of the the penalty [Zou and Li (2008)]. Such algorithms generate a solution sequence $\{\beta^k\}_k$ that can guarantee the convergence of the objective functions, but the convergence property of $\{\beta^k\}_k$ is generally unknown. Moreover, the cost per iteration of this type of algorithms is the cost of a LASSO solver. The second type of method includes coordinate descent (CD) type algorithms [Breheny and Huang (2011); Mazumder et al. (2011)]. The best convergence result for CD algorithms for minimizing (1.5) is that any cluster point of $\{\beta^k\}_k$ must be a stationary point of (1.6) and (1.7) [Breheny and Huang (2011); Mazumder et al. (2011)]. As shown in [Breheny and Huang

(2011); Mazumder et al. (2011)], CD-type algorithms are faster than the first type of algorithms mentioned above, because the cost per iteration of CD algorithms is only $O(np)$. However, when high accuracy is pursued CD-type algorithms may need lots of iterations, since its convergence speed is sub-linear numerically or linearly locally Li and Pong (2017).

In this paper we develop a local but superlinearly convergent algorithm for minimizing (1.5) with the SCAD and the MCP. To this end, we first establish that the global minimizers of (1.5) with the SCAD penalty (1.6) and MCP (1.7) are roots of the nonsmooth KKT equations. Conversely we show that any root of the KKT equations is at least a global coordinate-wise minimizer and stationary point of (1.5). Then we adopt Semi-smooth Newton (SSN) algorithm [Kummer (1988); Qi and Sun (1993); Ito and Kunisch (2008)] to solve the nonsmooth KKT equations. We establish the locally superlinear convergence property of SSN. Furthermore, computational complexity analysis shows that the cost of each iteration in SSN is at most $O(np)$, which is the same as coordinate descent. Hence, for a given λ, γ , the overall cost of using SSN to find a (local) minimizer of (1.5) is still $O(np)$, since SSN always converges after only a few iterations if it is warm-started. Thus SSN is possibly one of the fastest and most accurate algorithms for computing the whole solution path of (1.5) by running SSN repeatedly at some given $\lambda_k, k = 1, 2, \dots, M$ with warm start. Numerical simulation results comparing with CD algorithms also verify this.

The remainder of this paper is organized as follows. In Section 2 we describe the Semi-smooth Newton (SSN) algorithm. In Section 3 we establish the superlinear convergence property and analyze its computational complexity. Implementation detail and numerical comparison with coordinate descent (CD) algorithm on simulated and real data examples are given in Section 4. We conclude in Section 5 with comments and future work.

2 Semi-smooth Newton algorithm for penalized regression

2.1 Notation and background on Newton derivative

We first introduce the notation used throughout this paper and describe the concept and properties of Newton's derivative [Kummer (1988); Qi and Sun (1993); Chen et al. (2000); Ito and Kunisch (2008)].

With $\|\beta\|_q = (\sum_{i=1}^p |\beta_i|^q)^{\frac{1}{q}}$ we denote the usual q -norm ($q \in [1, \infty]$) of a column vector $\beta = (\beta_1, \beta_2, \dots, \beta_p)^T \in \mathbb{R}^p$, X^T is the transpose of the feature matrix $X \in \mathbb{R}^{n \times p}$, $\|X\|$ denotes the operator norm of X induced by the vector 2-norm. $\mathbf{1}$ or $\mathbf{0}$ denote a column vector or a matrix with elements all 1 or 0. Define $S = \{1, 2, \dots, p\}$. For any $A \subseteq S$ with length $|A|$, we

denote $\beta_A \in \mathbb{R}^{|A|}$ (or $X_A \in \mathbb{R}^{|A| \times p}$) as the subvector (or submatrix) whose entries (or columns) are listed in A . And X_{AB} denotes submatrix of X whose rows and columns are listed in A and B respectively. $\text{supp}(\beta)$ denotes the support of β , and $\text{sign}(z)$ denotes the sign of a given vector z .

Let $F : \mathbb{R}^m \rightarrow \mathbb{R}^l$ be a nonlinear map. [Kummer (1988); Qi and Sun (1993); Chen et al. (2000); Ito and Kunisch (2008)] generalized the classical Newton-Raphson algorithm to find a root of $F(z) = \mathbf{0}$, when F is not Fréchet differentiable but only Newton differentiable in the following sense.

Definition 2.1. $F : \mathbb{R}^m \rightarrow \mathbb{R}^l$ is called Newton differentiable at $x \in \mathbb{R}^m$ if there exists an open neighborhood $N(x)$ and a family of mappings $D : N(x) \rightarrow \mathbb{R}^{l \times m}$ such that

$$\|F(x+h) - F(x) - D(x+h)h\|_2 = o(\|h\|_2) \quad \text{for} \quad \|h\|_2 \rightarrow 0.$$

The set of mappings $\{D(z) : z \in N(x)\}$ denoted by $\nabla_N F(x)$ is called Newton derivative of F at x .

It can be easily seen that $\nabla_N F(x)$ coincides with the Fréchet derivative at x if F is continuously Fréchet differentiable. Let $F_i : \mathbb{R}^m \rightarrow \mathbb{R}^1$ be Newton differentiable at x with Newton derivative $\nabla_N F_i(x)$, $i = 1, 2, \dots, l$, then $F = (F_1, F_2, \dots, F_l)^T$ is also Newton differentiable at x with Newton derivative

$$\nabla_N F(x) = (\nabla_N F_1(x), \nabla_N F_2(x), \dots, \nabla_N F_l(x))^T. \quad (2.1)$$

Furthermore, if both F and H are Newton differentiable at x then any linear combination of them is also Newton differentiable at x , i.e., for any $\theta, \mu \in \mathbb{R}^1$

$$\nabla_N(\theta F + \mu G)(x) = \theta \nabla_N F(x) + \mu \nabla_N G(x) \quad (2.2)$$

Let $H : \mathbb{R}^s \rightarrow \mathbb{R}^l$ be Newton differentiable with Newton derivative $\nabla_N H$. Let $L \in \mathbb{R}^{s \times m}$ and define $F(x) = H(Lx + z)$ for any given $z \in \mathbb{R}^s$. Then it is easy to check by definition that the chain rule holds, i.e., $F(x)$ is Newton differentiable at x with Newton derivative

$$\nabla_N F(x) = \nabla_N H(Lx + z)L. \quad (2.3)$$

In Lemma 2.2 we will give two important thresholding functions which are Newton differentiable but not Fréchet differentiable.

2.2 Optimality conditions and Semi-smooth Newton algorithm

In this subsection, we give a necessary condition for the global minimizers of (1.5) with the SCAD penalty (1.6) and the MCP (1.7). Specifically, we show that the global minimizers satisfy

a set of KKT equations, which are nonsmooth but are Newton differentiable equations. Then we use Semi-smooth Newton algorithm to solve it.

Now we derive the optimality conditions of the minimizers of (1.5) with $p(z; \lambda, \gamma)$ to be $p_{scad}(z; \lambda, \gamma)$ or $p_{mcp}(z; \lambda, \gamma)$. This notation will be used in the rest of the paper for simplicity.

For a given $t \in \mathbb{R}^1$, let

$$T(t; \lambda, \gamma) = \arg \min_{z \in \mathbb{R}^1} \frac{1}{2}(z - t)^2 + p(z; \lambda, \gamma). \quad (2.4)$$

be the thresholding functions corresponding to penalty $p(z; \lambda, \gamma)$, which have a closed form for both SCAD and MCP penalties [Breheny and Huang (2011); Mazumder et al. (2011)].

Lemma 2.1. *Let $T(t; \lambda, \gamma)$ be defined in (2.4). Then for $p = p_{mcp}$,*

$$T_{mcp}(t; \lambda, \gamma) = \begin{cases} \frac{S(t; \lambda)}{1 - 1/\gamma}, & \text{if } |t| \leq \gamma\lambda, \\ t, & \text{if } |t| > \gamma\lambda. \end{cases} \quad (2.5)$$

and for $p = p_{scad}$,

$$T_{scad}(t; \lambda, \gamma) = \begin{cases} S(t; \lambda), & \text{if } |t| \leq 2\lambda, \\ \frac{S(t; \lambda\gamma/(\gamma - 1))}{1 - 1/(\gamma - 1)}, & \text{if } 2\lambda < |t| \leq \gamma\lambda, \\ t, & \text{if } |t| > \gamma\lambda. \end{cases} \quad (2.6)$$

respectively, where the scalar function $S(t; \lambda) = \max\{|t| - \lambda, 0\} \text{sign}(t)$ is the soft threshold function [Donoho and Johnstone (1995)].

Proof. See APPENDIX A. □

The following KKT condition shows that the global minimizers of (1.5) satisfy a nonsmooth equation which is the basis of our Semi-smooth Newton algorithm.

THEOREM 2.1. *Let $\hat{\beta}$ be a global minimizer of (1.5). Then there exists $\hat{d} \in \mathbb{R}^p$ such that the following optimality conditions hold,*

$$\hat{d} = \tilde{y} - G\hat{\beta}, \quad (2.7)$$

$$\hat{\beta} = \mathbb{T}(\hat{\beta} + \hat{d}; \lambda, \gamma). \quad (2.8)$$

where $G = X^T X$, $\tilde{y} = X^T y$, for a given vector $z \in \mathbb{R}^p$, $\mathbb{T}(z; \lambda, \gamma)$ is the thresholding operator operates on z component-wise by (2.4).

Conversely, if there exists $(\hat{\beta}, \hat{d})$ satisfying (2.7) - (2.8), then $\hat{\beta}$ is a stationary point of (1.5).

Proof. See APPENDIX B. □

Let

$$F(\beta; d) = \begin{bmatrix} F_1(\beta; d) \\ F_2(\beta; d) \end{bmatrix} : \mathbb{R}^p \times \mathbb{R}^p \rightarrow \mathbb{R}^{2p}, \quad (2.9)$$

where $F_1(\beta; d) := \beta - \mathbb{T}(\hat{\beta} + \hat{d}; \lambda, \gamma)$, and $F_2(\beta; d) := G\beta + d - \tilde{y}$. For simplicity, we refer to F as a KKT function. By Theorem 2.1, the global minimizers of (1.5) are roots of $F(\beta; d)$. And the roots of $F(\beta; d)$ are stationary points of (1.5). The difficulty is that the thresholding operators corresponding concave penalties include the SCAD and the MCP, F is not differentiable. So we resort to the semi-smooth Newton method (SSN) [Kummer (1988); Qi and Sun (1993); Chen et al. (2000); Ito and Kunisch (2008)].

Let $z = (\beta; d)$. At the k th iteration, the semi-smooth Newton method for finding the root of $F(z) = 0$ consists of two steps.

- (1) Solve $H^k \delta^k = -F(z^k)$ for δ^k , where H_k is an element of $\nabla_N F(z^k)$.
- (2) Update $z^{k+1} = z^k + \delta^k$, set $k \leftarrow k + 1$ and go to step (1).

This has the same form as the classical Newton method, except that here we use an element of $\nabla_N F(z^k)$ in step (1). Indeed, the key to the success of this method is to find a suitable and invertible H^k . We state this method in Algorithm 1.

Algorithm 1 Semi-smooth Newton algorithm for finding a root z^* of $F(z)$

- 1: Input: initial guess z^0 . Set $k = 0$.
- 2: **for** $k = 0, 1, 2, 3, \dots$ **do**
- 3: Choose $H^k \in \nabla_N F(z^k)$.
- 4: Get the Semi-smooth Newton direction δ^k by solving

$$H^k \delta^k = -F(z^k). \quad (2.10)$$

- 5: Update $z^{k+1} = z^k + \delta^k$.
 - 6: Stop or $k := k + 1$.
 - 7: **end for**
 - 8: Output: \hat{z} as a estimation of z^* .
-

2.3 The Newton derivatives of the KKT functions

Denote the KKT functions as defined in (2.9) by F_{scad} and F_{mcp} for the SCAD and the MCP, respectively. To compute the roots of F_{mcp} and F_{scad} based on the SSN, we need to calculate their Newton derivatives.

Lemma 2.2. $T_{mcp}(t; \lambda, \gamma)$ and $T_{scad}(t; \lambda, \gamma)$ are Newton differentiable with respect to t with Newton derivatives

$$\nabla_N T_{mcp}(t) = \begin{cases} 0, & |t| < \lambda, \\ r \in \mathbb{R}^1, & |t| = \lambda, \\ 1/(1-1/\gamma), & \lambda < |t| < \gamma\lambda, \\ r \in \mathbb{R}^1, & |t| = \gamma\lambda, \\ 1, & \gamma\lambda < |t|, \end{cases} \quad (2.11)$$

and

$$\nabla_N T_{scad}(t) = \begin{cases} 0, & |t| < \lambda, \\ r \in \mathbb{R}^1, & |t| = \lambda, \\ 1, & \lambda < |t| < 2\lambda, \\ r \in \mathbb{R}^1, & |t| = 2\lambda, \\ 1/(1-1/(\gamma-1)), & 2\lambda < |t| < \gamma\lambda, \\ r \in \mathbb{R}^1, & |t| = \gamma\lambda, \\ 1, & \gamma\lambda < |t|, \end{cases} \quad (2.12)$$

respectively.

Proof. See APPENDIX C. □

2.3.1 The Newton derivative of F_{mcp}

Consider the KKT function F_{mcp} . For any given point $z^k = (\beta^k; d^k) \in \mathbb{R}^{2p}$, define

$$A_k^1 = \{i \in S : \lambda < |\beta_i^k + d_i^k| < \lambda\gamma\}, \quad (2.13)$$

$$A_k^2 = \{i \in S : |\beta_i^k + d_i^k| \geq \lambda\gamma\}, \quad (2.14)$$

$$A_k = A_k^1 \cup A_k^2, \quad (2.15)$$

$$B_k = \{i \in S : |\beta_i^k + d_i^k| \leq \lambda\}. \quad (2.16)$$

We rearrange the order of the entries of z^k as follows:

$$z_{mcp}^k = (\beta_{A_k^1}^k; d_{A_k^2}^k; \beta_{B_k}^k; d_{A_k^1}^k; \beta_{A_k^2}^k; d_{B_k}^k).$$

Denote the Newton derivative of F_{mcp} at z_{mcp}^k as $\nabla_N F_{mcp}(z_{mcp}^k)$. In Theorem 2.2, we will show that $H_{mcp}^k \in \nabla_N F_{mcp}(z_{mcp}^k)$, where, $H_{mcp}^k \in \mathbb{R}^{p \times p}$ is given by

$$H_{mcp}^k = \begin{bmatrix} H_{11}^k & H_{12}^k \\ H_{21}^k & H_{22}^k \end{bmatrix} \quad (2.17)$$

with

$$H_{11}^k = \begin{bmatrix} -\frac{1}{\gamma-1}I_{A_k^1 A_k^1} & \mathbf{0} & \mathbf{0} \\ \mathbf{0} & -I_{A_k^2 A_k^2} & \mathbf{0} \\ \mathbf{0} & \mathbf{0} & I_{B_k B_k} \end{bmatrix}, \quad H_{12}^k = \begin{bmatrix} -\frac{\gamma}{\gamma-1}I_{A_k^1 A_k^1} & \mathbf{0} & \mathbf{0} \\ \mathbf{0} & \mathbf{0} & \mathbf{0} \\ \mathbf{0} & \mathbf{0} & \mathbf{0} \end{bmatrix},$$

$$H_{21}^k = \begin{bmatrix} G_{A_k^1 A_k^1} & \mathbf{0} & G_{A_k^1 B_k} \\ G_{A_k^2 A_k^1} & I_{A_k^2 A_k^2} & G_{A_k^2 B_k} \\ G_{B_k A_k^1} & \mathbf{0} & G_{B_k B_k} \end{bmatrix}, \quad H_{22}^k = \begin{bmatrix} I_{A_k^1 A_k^1} & G_{A_k^1 A_k^2} & \mathbf{0} \\ \mathbf{0} & G_{A_k^2 A_k^2} & \mathbf{0} \\ \mathbf{0} & G_{B_k A_k^2} & I_{B_k B_k} \end{bmatrix}.$$

2.3.2 The Newton derivative of F_{scad}

Now consider the KKT function F_{scad} . For any given point $z^k = (\beta^k; d^k) \in \mathbb{R}^{2p}$, define

$$A_k^1 = \{i \in S : \lambda < |\beta_i^k + d_i^k| < 2\lambda\}, \quad (2.18)$$

$$A_k^2 = \{i \in S : 2\lambda \leq |\beta_i^k + d_i^k| < \lambda\gamma\}, \quad (2.19)$$

$$A_k^3 = \{i \in S : |\beta_i^k + d_i^k| \geq \lambda\gamma\}, \quad (2.20)$$

$$A^k = A_k^1 \cup A_k^2 \cup A_k^3, \quad (2.21)$$

$$B_k = \{i \in S : |\beta_i^k + d_i^k| \leq \lambda\}. \quad (2.22)$$

We rearrange the entries of z_{scad} as follows:

$$z_{\text{scad}}^k := (\beta_{B_k}^k; d_{A_k^1}^k; \beta_{A_k^2}^k; d_{A_k^3}^k; d_{B_k}^k; \beta_{A_k^1}^k; d_{A_k^2}^k; \beta_{A_k^3}^k).$$

Denote the Newton derivative of F_{scad} at z_{scad}^k as $\nabla_N F_{\text{scad}}(z_{\text{scad}}^k)$. In Theorem 2.2, we will show that $H_{\text{scad}}^k \in \nabla_N F_{\text{scad}}(z_{\text{scad}}^k)$, where, $H_{\text{scad}}^k \in \mathbb{R}^{p \times p}$ is given by

$$H_{\text{scad}}^k := \begin{bmatrix} H_{11}^k & H_{12}^k \\ H_{21}^k & H_{22}^k \end{bmatrix} \quad (2.23)$$

with

$$H_{11}^k = \begin{bmatrix} I_{B_k B_k} & \mathbf{0} & \mathbf{0} & \mathbf{0} \\ \mathbf{0} & -I_{A_k^1 A_k^1} & \mathbf{0} & \mathbf{0} \\ \mathbf{0} & \mathbf{0} & -\frac{1}{\gamma-2}I_{A_k^2 A_k^2} & \mathbf{0} \\ \mathbf{0} & \mathbf{0} & \mathbf{0} & -I_{A_k^3 A_k^3} \end{bmatrix}, \quad H_{12}^k = \begin{bmatrix} \mathbf{0} & \mathbf{0} & \mathbf{0} & \mathbf{0} \\ \mathbf{0} & \mathbf{0} & \mathbf{0} & \mathbf{0} \\ \mathbf{0} & \mathbf{0} & -\frac{\gamma-1}{\gamma-2}I_{A_k^2 A_k^2} & \mathbf{0} \\ \mathbf{0} & \mathbf{0} & \mathbf{0} & \mathbf{0} \end{bmatrix},$$

$$H_{21}^k = \begin{bmatrix} G_{B_k B_k} & \mathbf{0} & G_{B_k A_k^2} & \mathbf{0} \\ G_{A_k^1 B_k} & I_{A_k^1 A_k^1} & G_{A_k^1 A_k^2} & \mathbf{0} \\ G_{A_k^2 B_k} & \mathbf{0} & G_{A_k^2 A_k^2} & \mathbf{0} \\ G_{A_k^3 B_k} & \mathbf{0} & G_{A_k^3 A_k^2} & I_{A_k^3 A_k^3} \end{bmatrix}, \quad H_{22}^k = \begin{bmatrix} I_{B_k B_k} & G_{B_k A_k^1} & \mathbf{0} & G_{B_k A_k^3} \\ \mathbf{0} & G_{A_k^1 A_k^1} & \mathbf{0} & G_{A_k^1 A_k^3} \\ \mathbf{0} & G_{A_k^2 A_k^1} & I_{A_k^2 A_k^2} & G_{A_k^2 A_k^3} \\ \mathbf{0} & G_{A_k^3 A_k^1} & \mathbf{0} & G_{A_k^3 A_k^3} \end{bmatrix}.$$

THEOREM 2.2. Both F_{mcp} and F_{scad} are Newton differentiable at z_{mcp}^k and z_{scad}^k with

$$H_{mcp}^k \in \nabla_N F_{mcp}(z_{mcp}^k),$$

and

$$H_{scad}^k \in \nabla_N F_{scad}(z_{scad}^k).$$

Furthermore, the inverse of H_{mcp}^k and H_{scad}^k are uniformly bounded with

$$\|(H_{mcp}^k)^{-1}\| \leq M_\gamma,$$

and

$$\|(H_{scad}^k)^{-1}\| \leq M_\gamma,$$

where, $M_\gamma = (3\gamma + 2) + (\gamma + 1)(2\gamma + 5)$.

Proof. See APPENDIX D. □

With the Newton derivative at hand we can apply SSN to compute the roots of F_{mcp} and F_{scad} . Here we give the details for F_{mcp} . By the definitions of A_k^1, A_k^2, I_k and T_{mcp} , we get

$$F_{mcp}(z_{mcp}^k) = \begin{bmatrix} \beta_{A_k^1}^k - \frac{\gamma}{\gamma-1}(\beta_{A_k^1}^k + d_{A_k^1}^k - \lambda \text{sign}(\beta_{A_k^1}^k + d_{A_k^1}^k)) \\ \beta_{A_k^2}^k - (\beta_{A_k^2}^k + d_{A_k^2}^k) \\ \beta_{B_k}^k \\ G_{A_1^k A_1^k} \beta_{A_1^k}^k + G_{A_1^k A_2^k} \beta_{A_2^k}^k + G_{A_1^k B_k} \beta_{B_k}^k + d_{A_1^k}^k - \tilde{y}_{A_1^k} \\ G_{A_k^2 A_k^1} \beta_{A_k^1}^k + G_{A_k^2 A_k^2} \beta_{A_k^2}^k + G_{A_k^2 B_k} \beta_{B_k}^k + d_{A_k^2}^k - \tilde{y}_{A_k^2} \\ G_{B_k A_k^1} \beta_{A_k^1}^k + G_{B_k A_k^2} \beta_{A_k^2}^k + G_{B_k B_k} \beta_{B_k}^k + d_{B_k}^k - \tilde{y}_{B_k} \end{bmatrix}. \quad (2.24)$$

Substituting (2.24) and (2.17) into the Semi-smooth Newton direction equation

$$H_{mcp}^k \delta_{mcp}^k = -F_{mcp}(z_{mcp}^k)$$

and observing the update relation

$$z_{mcp}^{k+1} = z_{mcp}^k + \delta_{mcp}^k,$$

we get (after some tedious algebraic simplifications)

$$d_{A_k^2}^{k+1} = \mathbf{0}, \quad (2.25)$$

$$\beta_{B_k}^{k+1} = \mathbf{0}, \quad (2.26)$$

$$\tilde{G}_{A_k A_k} \beta_{A_k}^{k+1} = s_{A_k}, \quad (2.27)$$

$$d_{A_k^1}^{k+1} = -\beta_{A_k^1}^{k+1} / \gamma + s_{A_k^1}, \quad (2.28)$$

$$d_{B_k}^{k+1} = \tilde{y}_{B_k} - G_{B_k A_k} \beta_{A_k}^{k+1}, \quad (2.29)$$

where,

$$\tilde{G}_{A_k A_k} = G_{A_k A_k} - \begin{bmatrix} I_{A_k^1 A_k^1} / \gamma & \mathbf{0} \\ \mathbf{0} & \mathbf{0} \end{bmatrix}, \quad (2.30)$$

$$s_{A_k^1} = \lambda \text{sign}(\beta_{A_k^1}^k + d_{A_k^1}^k), \quad (2.31)$$

$$s_{A_k} = \tilde{y}_{A_k} - \begin{bmatrix} s_{A_k^1} \\ \mathbf{0} \end{bmatrix}. \quad (2.32)$$

We summarize the above in the following algorithm.

Algorithm 2 Semi-Smooth Newton algorithm for finding a root of F_{mcp}

- 1: Input: X, y, λ, γ , initial guess $(\beta^0; d^0)$. Set $k = 0$.
 - 2: Pre-compute $\tilde{y} = X^T y$ and store it.
 - 3: **for** $k = 0, 1, 2, 3, \dots$ **do**
 - 4: Compute A_k^1, A_k^2, A_k, B_k by (2.13) - (2.16).
 - 5: $\beta_{B_k}^{k+1} = \mathbf{0}$.
 - 6: $d_{A_k^2}^{k+1} = \mathbf{0}$.
 - 7: Compute $\tilde{G}_{A_k A_k}, s_{A_k^1}, s_{A_k}$ by (2.30)-(2.32).
 - 8: $\beta_{A_k}^{k+1} = \tilde{G}_{A_k A_k}^{-1} s_{A_k}$.
 - 9: $d_{A_k^1}^{k+1} = -\beta_{A_k^1}^{k+1} / \gamma + s_{A_k^1}$,
 - 10: $d_{B_k}^{k+1} = \tilde{y}_{B_k} - G_{B_k A_k} \beta_{A_k}^{k+1}$.
 - 11: Check Stop condition
 - If stop
 - Denote the last iteration by $\beta_{\hat{A}}, \beta_{\hat{B}}, d_{\hat{A}}, d_{\hat{B}}$.
 - Else
 - $k := k + 1$.
 - 12: **end for**
 - 13: Output: $\hat{\beta} = (\beta_{\hat{A}}; \beta_{\hat{B}}), \hat{d} = (d_{\hat{A}}; d_{\hat{B}})$.
-

The Semi-smooth Newton algorithm for F_{scad} can be constructed in a similar fashion. Let

$$\tilde{G}_{A_k A_k} := G_{A_k A_k} - \begin{bmatrix} \mathbf{0} & \mathbf{0} & \mathbf{0} \\ \mathbf{0} & I_{A_k^2 A_k^2} / (\gamma - 1) & \mathbf{0} \\ \mathbf{0} & \mathbf{0} & \mathbf{0} \end{bmatrix}, \quad (2.33)$$

$$s_{A_k^2} := \frac{\gamma \lambda}{\gamma - 1} \text{sign}(\beta_{A_k^2}^k + d_{A_k^2}^k), \quad (2.34)$$

$$s_{A_k} := \tilde{y}_{A_k} - \begin{bmatrix} d_{A_k^1}^{k+1} \\ s_{A_k^2} \\ \mathbf{0} \end{bmatrix}. \quad (2.35)$$

Then the algorithm for solving $F_{\text{scad}}(z) = 0$ is as follows.

Algorithm 3 Semi-Smooth Newton algorithm for finding a root of F_{scad}

- 1: Input: X, y, λ, γ , initial guess $(\beta^0; d^0)$. Set $k = 0$.
 - 2: Pre-compute $\tilde{y} = X^T y$ and store it.
 - 3: **for** $k = 0, 1, 2, 3, \dots$ **do**
 - 4: Compute $A_k^1, A_k^2, A_k^3, A_k, B_k$ by (2.18) - (2.22).
 - 5: $\beta_{B_k}^{k+1} = \mathbf{0}$.
 - 6: $d_{A_k^1}^{k+1} = \lambda \text{sign}(\beta_{A_k^1}^k + d_{A_k^1}^k)$.
 - 7: $d_{A_k^3}^{k+1} = \mathbf{0}$.
 - 8: Compute $\tilde{G}_{A_k A_k}, s_{A_k^2}, s_{A_k}$ by (2.33)-(2.35).
 - 9: $\beta_{A_k}^{k+1} = \tilde{G}_{A_k A_k}^{-1} s_{A_k}$.
 - 10: $d_{A_k^2}^{k+1} = -\beta_{A_k^2}^{k+1} / (\gamma - 1) + s_{A_k^2}$,
 - 11: $d_{B_k}^{k+1} = \tilde{y}_{B_k} - G_{B_k A_k} \beta_{A_k}^{k+1}$.
 - 12: Check Stop condition
 - If stop
 - Denote the last iteration by $\beta_{\hat{A}}, \beta_{\hat{B}}, d_{\hat{A}}, d_{\hat{B}}$.
 - Else
 - $k := k + 1$.
 - 13: **end for**
 - 14: Output: $\hat{\beta} = (\beta_{\hat{A}}; \beta_{\hat{B}}), \hat{d} = (d_{\hat{A}}; d_{\hat{B}})$.
-

A natural stopping criterion for both algorithms is when $A_k = A_{k+1}$ holds for some k , which can be checked inexpensively. We also stop them when the iteration k exceeds some given positive integer J as a safeguard.

Remark 2.1. *It is obvious that Algorithm 2 and Algorithm 3 are well-defined if $\tilde{G}_{A_k A_k}$ in (2.30) and (2.33) are invertible respectively. Sufficient conditions to guarantee these are*

$$\gamma > 1/\kappa_-(|A_k|), \quad (2.36)$$

$$\gamma > 1 + 1/\kappa_-(|A_k|), \quad (2.37)$$

respectively, where

$$\kappa_{-}(|A_k|) = \min_{\|z\|=1, \|z\|_0 \leq |A_k|} \|Xz\|^2$$

denotes the lower sparse eigenvalues of X with order $|A_k|$ [Zhang and Huang (2008)]. Hence under the common assumption that $\kappa_{-}(c\|\beta^\dagger\|_0)$ (c is a small integer) is bounded away from 0 and the concavity parameter γ are large enough both (2.36) and (2.37) will hold.

3 Convergence, complexity analysis and solution path

In this subsection, following [Kummer (1988); Qi and Sun (1993); Chen et al. (2000); Ito and Kunisch (2008)], we will establish the local superlinear convergence result of Algorithms 2 and 3, which are similar to the classical Newton algorithm, and analyze their computational complexity.

3.1 Convergence

THEOREM 3.1. *Let β_{mcp}^k and β_{scad}^k be generated by Algorithms 2 and 3, respectively. Then, β_{mcp}^k and β_{scad}^k converge locally and superlinearly to point satisfying equation (2.7) - (2.8).*

Proof. See APPENDIX E. □

Remark 3.1. *By Theorem 2.1 we can see Algorithms 2 and 3 also converge locally and superlinearly to a stationary points of (1.5) with the MCP (1.7) and SCAD penalty (1.6), respectively.*

3.2 Computational complexity

We now consider the number of floating point operations per iteration. It takes $O(p)$ flops to finish step 4-7 (step 4-8) in Algorithm 2 (Algorithm 3). For step 8 (step 9) in Algorithm 2 (Algorithm 3), inverting the positive definite matrix $\tilde{G}_{A_k A_k}$ by Cholesky factorization takes $O(|A_k|^3)$ flops. As for step 9-10 (10-11) in Algorithm 2 (Algorithm 3), $O(np)$ flops are enough to finish the matrix-vector product. So the overall cost per iteration for Algorithms 2 and Algorithm 3 is $O(\max(|A_k|^3, pn))$. Numerically $|A_k|$ usually increases and converges to $O(\|\beta^\dagger\|_0)$ if the algorithm is warm started. Therefore, if the underlying solution is sufficiently sparse such that $\|\beta^\dagger\|_0^3 \leq O(np)$ then it takes $O(np)$ flops per iteration for both algorithms. Hence the overall cost of Algorithms 2 and 3 are still $O(np)$ due to their superlinear convergence. The computational complexity analysis shows that it is very fast to use Algorithm 2 and 3 to compute the solution paths with warm starts. This is supported by the numerical results presented in Section 4.

The computational cost of coordinate descent algorithm [Breheny and Huang (2011); Mazumder et al. (2011)] and iterative thresholding algorithm [She (2009)] for (1.6) and (1.7) is also $O(np)$

per iteration. The cluster points of sequences generated by CD and iterative thresholding also satisfy (2.7)-(2.8). But the convergence rate of these two type of algorithms is at best sub-linear even in the case of lasso penalized problem where the object function is convex [Beck and Teboulle (2009)]. Hence it is not surprising that Algorithms 2 and 3 outperform CD-type algorithms in accuracy and efficiency, see, numerical results in Section 4.

3.3 Solution path

An important issue in implementing a Newton-type algorithm is how to choose an initial value. We use warm start to determine the initial value. This strategy has been successfully used for computing the Lasso and the Enet paths [Friedman et al. (2007)]. It is also a simple but powerful tool to handle the local convergence of concavely penalized regression problems [Breheny and Huang (2011); Mazumder et al. (2011); Jiao et al. (2015)]. Hence we use warm start to generate the solution path on an interval of the penalty parameter λ . The locally superlinear convergence results in Theorem 3.1 guarantee that after a small number of iterations we will get an approximate solution with high accuracy if the algorithms are warm started.

We are also often interested in the whole solution path $\hat{\beta}(\lambda)$ for $\lambda \in [\lambda_{\min}, \lambda_{\max}]$, where $0 < \lambda_{\min} < \lambda_{\max}$ are two prespecified numbers. This will be needed for selecting the λ value based on a data driven procedure such as cross validation or bayesian information criterion. Here we approximate the solution path by computing $\hat{\beta}(\lambda)$ on a given finite set $\Lambda = \{\lambda_0, \lambda_1, \dots, \lambda_M\}$ for some integer M , where $\lambda_0 > \dots > \lambda_M > 0$. Obviously, $\hat{\beta}(\lambda) = \mathbf{0}$ satisfies (2.7) and (2.8) if $\lambda \geq \|X'y\|_{\infty}$. Hence we set $\lambda_{\max} = \lambda_0 = \|X'y\|_{\infty}$, $\lambda_t = \lambda_0 \gamma^t$, $t = 0, 1, \dots, M$, and $\lambda_{\min} = \lambda_0 \gamma^M$, where $\gamma \in (0, 1)$. We use the solution at λ_t as the initial value for computing the solution at λ_{t+1} .

To decide the ‘‘optimal’’ choice of λ , a high-dimensional Bayesian information criterion (HBIC) [Wang et al. (2013); Shi et al. (2018)] can be utilized. In this paper, we also propose to use a novel voting selection criterion (VSC) [Huang et al. (2017, 2018)] for choosing the optimal value of tuning parameter. Assume we run the SSN Algorithm to yield a solution path until $\|\hat{\beta}_{\lambda_t}\|_0 > \lfloor n/\log(p) \rfloor$ on the sequence $\{\lambda_t\}$. Let

$$\Lambda_{\ell} = \{\lambda_t : \|\hat{\beta}_{\lambda_t}\|_0 = \ell, t = 1, \dots, M\},$$

where $\ell = 1, \dots, \lfloor n/\log(p) \rfloor$ is the set of tuning parameter at which the output of SSN has ℓ nonzero elements. Then we determine λ by VSC as

$$\hat{\lambda} = \max_{\ell} \{\Lambda_{\ell}\} \quad \text{and} \quad \bar{\ell} = \arg \max_{\ell} \{|\Lambda_{\ell}|\}. \quad (3.1)$$

It is noteworthy that the VSC selector is seamlessly integrated with the warmstarting technique without any extra computational overhead.

Remark 3.2. *Both the HBIC and the VSC selectors work well in our numerical examples. When the assumption of linear model is satisfied, numerical results show that VSC is slightly more accurate than HBIC. Thus one can use either HBIC or VSC to find a solution for simulated data, while it is suggested to use the HBIC for real-world data.*

4 Numerical Examples

In this section we present numerical examples to illustrate the performance of the proposed SSN algorithm. All the experiments are performed in MATLAB R2010b and R version 3.3.2 on a quad-core laptop with an Intel Core i5 CPU (2.60 GHz) and 8 GB RAM running Windows 8.1 (64 bit).

4.1 Implementation Setting

We generate synthetic data from (1.1). The rows of the $n \times p$ matrix X are sampled as i.i.d. copies from $N(\mathbf{0}, \Sigma)$ with $\Sigma = (r^{|j-k|})$, $1 \leq j, k \leq p$, where r is the correlation coefficient of X . The noise vector ε is generated independently from $N(\mathbf{0}, \sigma^2 I_n)$, where σ is the noise level. The underlying regression coefficient vector β^\dagger is a random sparse vector chosen as T -sparse with a dynamic range (DR) given by

$$\text{DR} := \frac{\max\{|\beta_j^\dagger| : \beta_j^\dagger \neq 0\}}{\min\{|\beta_j^\dagger| : \beta_j^\dagger \neq 0\}} = 10. \quad (4.1)$$

Let $\mathcal{A} = \{j : \beta_j^\dagger \neq 0\}$ be the true model and $\widehat{\mathcal{A}} = \{j : \widehat{\beta}_j \neq 0\}$ be the estimated model. Following Becker et al. (2011), each nonzero entry of β^\dagger is generated as follows:

$$\beta_j^\dagger = \eta_{1j} 10^{\eta_{2j}}, \quad (4.2)$$

where $j \in \mathcal{A}$, $\eta_{1j} = \pm 1$ with probability $\frac{1}{2}$ and η_{2j} is uniformly distributed in $[0, 1]$. Then the outcome vector y is generated via $y = X\beta^\dagger + \varepsilon$.

We compare our SSN algorithm with the CD algorithm in Breheny and Huang (2011) for solving (1.5), which is summarized in Algorithm 4. The stopping criterion at step 8 of Algorithm 4 is chosen to be either $k \geq J$ or $\|\beta^{k+1} - \beta^k\| \leq \delta$ with $\delta = 1e - 3$.

For SCAD and MCP, to improve computing efficiency, we fix $\gamma = 3.7$ and $\gamma = 2.7$ as suggested by Fan and Li (2001) and Zhang (2010a) respectively throughout this paper. For simulation studies, λ tuning parameters are selected by VSC. In real data examples, we use the HBIC tuning parameter selector.

Algorithm 4 CD for MCP or SCAD

- 1: Input: X, y, λ, γ , initial guess β^0 and $r^0 = y - X\beta^0$. Set $k = 0$.
 - 2: **for** $k = 0, 1, 2, 3, \dots$ **do**
 - 3: **for** $j = 1, 2, \dots, p$ **do**
 - 4: Calculate $z_j^k = X_j^T r^k + \beta_j^k$, where X_j is the j th column of X and $r^k = y - X\beta^k$ is the current residual value.
 - 5: Update $\beta_j^{k+1} \leftarrow T_{\text{mcp}}(z_j^k; \lambda, \gamma)$ or $\beta_j^{k+1} \leftarrow T_{\text{scad}}(z_j^k; \lambda, \gamma)$.
 - 6: Update $r^{k+1} \leftarrow r^k - (\beta_j^{k+1} - \beta_j^k)X_j$.
 - 7: **end for**
 - 8: Check Stop condition
 If stop
 Denote the last iteration by $\hat{\beta}$.
 Else
 $k := k + 1$.
 - 9: **end for**
 - 10: Output: $\hat{\beta}$.
-

4.2 Simulation

4.2.1 Efficiency and Accuracy

We set $p = 1000$ and 2000 with $n = \lfloor p/5 \rfloor$ and $T = \lfloor n/[2 \log(p)] \rfloor$, where $\lfloor x \rfloor$ denotes the integer part of x for $x \geq 0$. We choose three levels of correlation $r = 0.3, 0.5$ and 0.7 , which correspond to the weak, moderate and strong correlation. We consider two levels of noise: $\sigma = 1$ (higher level) and $\sigma = 0.1$ (lower level). The number of simulations is $N = 100$.

To further illustrate the efficiency and accuracy of the proposed SSN algorithm, based on N replications, we compare it with the CD algorithm in terms of the average CPU time (Time, in seconds), the average estimated model size (MS) $N^{-1} \sum_{m=1}^N |\hat{\mathcal{A}}^{(m)}|$, the proportion of correct models (CM) $N^{-1} \sum_{m=1}^N I\{\hat{\mathcal{A}}^{(m)} = \mathcal{A}\}$ (in percentage terms), the average ℓ_∞ absolute error $N^{-1} \sum_{m=1}^N \|\hat{\beta}^{(m)} - \beta^\dagger\|_\infty$ (AE) and the average ℓ_2 relative error $N^{-1} \sum_{m=1}^N (\|\hat{\beta}^{(m)} - \beta^\dagger\|_2 / \|\beta^\dagger\|_2)$ (RE). The above measures MS, CM, AE and RE evaluate the quality (accuracy) of the solutions. Clearly, the closer MS approaches to T , the closer CM approaches to 100%, and the smaller AE and RE, the higher the solution quality. Simulation results are summarized in Table 1.

For each (p, r, σ) combination, we see from Table 1 that SSN has better speed performance than CD for both MCP and SCAD, and SSN is about $3 \sim 9$ times faster than CD. In particular, for given penalty and algorithm, CPU time decreases as σ increases, increases linearly with

p , and is fairly robust to the choice of r . For SCAD, SSN and CD are comparable in terms of solution quality. Unsurprisingly, larger σ will degrade the accuracy for both CD and SSN. When the correlation level is low or moderate (i.e., $r = 0.3$ or 0.5), similar phenomena hold for MCP. For MCP with high correlation data (i.e., $r = 0.7$), CD provides a more accurate solution than SSN does, which is due to the choice of $\gamma = 2.7$ for MCP. In fact, simulations not reported in Table 1 show that if we increase the value of γ for MCP, say $\gamma = 4$, SSN can also produce similar solution quality comparing with CD. Please also refer to Remark 2.1 for relevant discussion. Overall, the simulation results in Table 1 show that SSN outperforms CD in terms of CPU time while producing solutions of comparable quality.

MCP or SCAD has a free parameter γ that controls its concavity. It is important to study the sensitivity of the proposed algorithm with respect to the variation of γ . In next subsection, we conduct the sensitivity analysis for γ and other model parameters.

4.2.2 Influence of Model Parameters

We now consider the effects of each of the model parameters ($\gamma, n, p, r, \sigma, T$) on the performance of SSN and CD more closely in terms of the exact support recovery probability (Probability), i.e., the percentage of $\widehat{\mathcal{A}}$ agrees with \mathcal{A} , and the CPU time (Time, in seconds). For the sake of simplicity, we consider γ for MCP and SCAD both, while (n, p, r, σ, T) for SCAD only, since similar variation tendency of the parameters happens for MCP. Results of Probability and Time averaged over 10 independent runs are given in Figure 1 and Figure 2, respectively. The parameters for solvers are set as follows.

Influence of the concavity parameter γ Data are generated from the model with ($\gamma \in \{1.1, 2.7, 5, 10, 20\}, n = 100, p = 500, r = 0.1, \sigma = 0.1, T = 10$) for MCP and ($\gamma \in \{2.1, 3.7, 5, 10, 20\}, n = 100, p = 500, r = 0.1, \sigma = 0.1, T = 10$) for SCAD.

Influence of the sample size n Data are generated from the model with ($\gamma = 3.7, n = 60 : 10 : 100, p = 500, r = 0.1, \sigma = 0.1, T = 10$).

Influence of the dimension p Data are generated from the model with ($\gamma = 3.7, n = 100, p = 500 : 500 : 2500, r = 0.1, \sigma = 0.1, T = 10$).

Influence of the correlation level r Data are generated from the model with ($\gamma = 3.7, n = 100, p = 500, r = 0.1 : 0.1 : 0.9, \sigma = 0.1, T = 10$).

Influence of the noise level σ Data are generated from the model with ($\gamma = 3.7, n = 100, p = 500, r = 0.1, \sigma \in \{0.2, 0.4, 0.8, 1.6, 3.2\}, T = 10$).

Influence of the sparsity level T Data are generated from the model with ($\gamma = 3.7, n = 100, p = 500, r = 0.1, \sigma = 0.1, T = 5 : 5 : 30$).

In summary, the results shown in Figure 1 and Figure 2 demonstrate that two solvers generally have similar variation tendency with considered model parameters, and SSN is considerably faster than CD while reaching better (or comparable) accuracy, which is consistent with the simulation results in Table 1. In particular, it is nice to see that the CPU time of SSN is insensitive to each of the model parameters ($\gamma, n, p, r, \sigma, T$) in Figure 2.

4.3 Application

4.3.1 Eye Disease Data Example

We analyze an eye disease data (eyedata) set which is publicly available in R package **flare** [Li et al. (2015)] to illustrate the application of the SSN in high-dimensional settings. This data set is a gene expression data from the microarray experiments of mammalian eye tissue samples of Scheetz et al. (2006) and is detailedly described and applied by many papers [Huang et al. (2008, 2016); Breheny and Huang (2015)] that want to find the gene probes that are most related to TRIM32 in sparse high-dimensional regression models. The response variable y is a numeric vector of length 120 giving expression level of gene TRIM32 which causes Bardet-Biedl syndrome (BBS). The design matrix X is a 120×200 matrix which represents the data of 120 rats with 200 gene probes.

Since the exact solution for the eyedata set is unknown, we consider three gold standards for comparison purposes: **flare**[Li et al. (2015)](the SQRT Lasso with $\lambda = \sqrt{\log(p)/n}$), **glmnet**[Friedman et al. (2010)] (10-fold cv.glmnet with the `lambda.1se` rule and `set.seed=0`) and **ncvreg** [Breheny and Huang (2011)] (10-fold cv.ncvreg with `seed=0`). Probe information, corresponding nonzero estimates, CPU time (Time) and predictive mean squared errors (PMSE) calculated by $n^{-1} \sum_{i=1}^n (\hat{y}_i - y_i)^2$ are provided in Table 2. From Table 2, accurate to 4 decimal places, **flare**, **glmnet**, **ncvreg**, MCP-CD, MCP-SSN, SCAD-CD and SCAD-SSN identify 18, 19, 5, 3, 6, 11 and 3 probes, respectively. The seven sets of identified probes have 3 in common, namely Probe 25141, Probe 28680 and Probe 28967. Although the magnitudes of estimates are not equal, they have the same signs, which suggests similar biological conclusions. Notably, comparing with other competitors, the proposed SSN has better speed performance while producing comparable PMSE.

4.3.2 Breast Cancer Data Example

We analyze the breast cancer data which comes from breast cancer tissue samples deposited to The Cancer Genome Atlas (TCGA) project and compiles results obtained using Agilent mRNA expression microarrays to illustrate the application of the SSN in high-dimensional settings. This data, which is named bcTCGA, is available at <http://myweb.uiowa.edu/pbreheny/data/bcTCGA.RData>. In this bcTCGA dataset, we have expression measurements of 17814 genes from 536 patients (all expression measurements are recorded on the log scale). There are 491 genes with missing data, which we have excluded. We restrict our attention to the 17323 genes without missing values. The response variable \mathbf{y} measures one of the 17323 genes, a numeric vector of length 536 giving expression level of gene BRCA1, which is the first gene identified that increases the risk of early onset breast cancer, and the design matrix \mathbf{X} is a 536×17322 matrix, which represents the remaining expression measurements of 17322 genes. Because BRCA1 is likely to interact with many other genes, it is of interest to find genes with expression levels related to that of BRCA1.

We consider an adaptive LASSO (ALASSO) [Zou (2006)] procedure using the `ncvreg` and `glmnet` packages in R for bcTCGA as the gold standard in comparison with SSN and CD. The following commands complete the main part of the ALASSO computation:

```
ptm <- proc.time()
library(ncvreg); fit <- ncvreg(X, y, penalty = 'lasso')
beta0 <- coef(fit, which=which.min(BIC(fit)))[-1]
weight <- abs(beta0)^(-1); weight <- pmin(weight, 1e10)
library(glmnet); set.seed(0)
cvfit <- cv.glmnet(X, y, nfolds=10, penalty.factor=weight)
betahat <- coef(cvfit, s = 'lambda.1se')
ptm <- (proc.time()-ptm)[3]
```

Gene information, corresponding nonzero estimates, CPU time and PMSE are provided in Table 3. From Table 3, accurate to 4 decimal places, ALASSO, MCP-CD, MCP-SSN, SCAD-CD and SCAD-SSN identify 8, 3, 6, 13 and 8 genes, respectively. We observe that some genes, such as C17orf53, CDC25C, DTL, NBR2, SPAG5 and VPS25, are selected by at least three solvers, and in particular, all methods capture the genes DTL and NBR2. NBR2 is adjacent to BRCA1 on chromosome 17, and recent experimental evidence indicates that the two genes share a promoter [Breheny (2017)]. It is also observed from Table 3 that SSN is about $11 \sim 15$ times faster than CD while producing smaller PMSE, which demonstrates the power of SSN to

identify the important biological factors from a large volume of noisy data.

5 Conclusion

Starting from the KKT condition we developed Semi-smooth Newton (SSN) algorithm for the MCP and SCAD regularized linear regression problem in high dimensional settings. We established the local superlinear convergence of SSN and analyzed its computational complexity. Combining the VSC or HBIC tuning parameter selector with warm start we obtain the solution path and select the tuning parameters in a fast and stable way. Numerical comparison with coordinate descent algorithm on simulated and real data sets showed that SSN is much faster than CD. We make all these innovations publicly available by developing a Matlab package named *ssn-nonconvex* available at <http://faculty.zuel.edu.cn/tjyjxxy/jyl/list.htm/>.

We will generalize SSN to group MCP/ SCAD or to regression problems with other loss functions in our future work. Semi-smooth Newton methods converges superlinearly but locally, we adopt simple continuation strategy to globalize it. Globalization via smoothing Newton methods Chen et al. (1998); Qi and Sun (1999); Qi et al. (2000) is also of immense interest.

Acknowledgment

Yuling Jiao is partially supported by the National Natural Science Foundation of China No. 11501579, and Yueyong Shi is partially supported by the National Natural Science Foundation of China Nos. 11501578 and 11701571.

Appendices

APPENDIX A: Proof of Lemma 2.1

Proof: See Breheny and Huang (2011) and Mazumder et al. (2011).

APPENDIX B: Proof of Theorem 2.1

Proof: Here we give the proof for the results for MCP since the proof for SCAD penalty is similar. Let $\hat{\beta} \in \mathbb{R}^p$ be a global minimizer of

$$E_{mcp}(\beta) := \frac{1}{2} \|X\beta - y\|_2^2 + \sum_{j=1}^p p_{mcp}(\beta_j; \lambda, \gamma).$$

Define

$$f_i(t) = E_{mcp}(\hat{\beta}_1, \dots, \hat{\beta}_{i-1}, t, \hat{\beta}_{i+1}, \dots, \hat{\beta}_p), i = 1, 2, \dots, p.$$

Then, by definition $\hat{\beta}_i$ is a global minimizer of the scalar function $f_i(t)$. Some algebra shows that the minimizer of $f_i(t)$ is also the minimizer of $\frac{1}{2}(t - (\hat{\beta}_i + X_i'(y - X\hat{\beta})))^2 + p_{\text{mcp}}(t; \lambda, \gamma)$. Then $\hat{\beta}_i = T_{\text{mcp}}(\hat{\beta}_i + X_i'(y - X\hat{\beta}); \lambda, \gamma)$ by Lemma 2.1. (2.7) - (2.8) follow from the definition of $G = X^T X$, $\tilde{y} = X^T y$ and $\mathbb{T}(\cdot; \lambda, \gamma)$.

Conversely, assume that $(\hat{\beta}, \hat{d})$ satisfying (2.7) - (2.8). Then $\forall i, \hat{\beta}_i = T_{\text{mcp}}(\hat{\beta}_i + X_i'(y - X\hat{\beta}); \lambda, \gamma)$ which implies that $\hat{\beta}_i$ is a minimizer of the $f_i(t)$ defined above. This shows $\hat{\beta}$ is a coordinate-wise minimizer of E_{mcp} . By Lemma 3.1 in Tseng (2001), $\hat{\beta}$ is also a stationary point.

APPENDIX C: Proof of Lemma 2.2

Proof: Observing that both $T_{\text{scad}}(\cdot; \lambda, \gamma)$ and $T_{\text{mcp}}(\cdot; \lambda, \gamma)$ are piecewise linear function on \mathbb{R}^1 , it suffices to prove that the piecewise linear scalar function

$$f(t) = \begin{cases} k_1 t + b_1, & \text{if } t \leq t_0, \\ k_2 t + b_2, & \text{if } t > t_0. \end{cases}$$

is Newton differentiable with

$$\nabla_N f(t) = \begin{cases} k_1, & t < t_0, \\ r \in \mathbb{R}^1, & t = t_0, \\ k_2, & t_0 < t. \end{cases} \quad (\text{A.1})$$

where k_1, k_2, b_1, b_2, t_0 are arbitrary such that $k_1 t_0 + b_1 = k_2 t_0 + b_2$. Indeed, let

$$D(t+h)h = \begin{cases} k_1 h, & t < t_0, \\ k_2 h, & t_0 < t, \end{cases}$$

and $G(t_0)h = rh$ with an arbitrary $r \in \mathbb{R}$, then $|f(t+h) - f(t) - D(t+h)h|/|h| \rightarrow 0$ as $|h| \rightarrow 0$.

APPENDIX D: Proof of Theorem 2.2

Proof: Here we give the proof for the results for MCP since the proof for SCAD penalty is sim-

ilar. Let $b(t; \lambda, \gamma) = \begin{cases} 0, & |t| \leq \lambda, \\ 1/(1-1/\gamma), & \lambda < |t| < \gamma\lambda, \\ 1, & \gamma\lambda \geq |t|, \end{cases}$ $\mathbf{b}(x; \lambda, \gamma) = \text{diag}[b(x_1; \lambda, \gamma), \dots, b(x_p; \lambda, \gamma)]'$, $g_i(x) = T_{\text{mcp}}(e_i' x; \lambda, \gamma) : x \in \mathbb{R}^p \rightarrow \mathbb{R}^1, i = 1, \dots, p$, where the column vector e_i is the i th orthonormal basis in \mathbb{R}^p , $\mathbb{T}(x; \lambda, \gamma) = [g_1(x), \dots, g_p(x)]'$. It follows Lemma 2.2 and (2.1)-(2.3) that $b(t; \lambda, \gamma) \in \nabla_N T_{\text{mcp}}(t)$ and

$$\mathbf{b}(x; \lambda, \gamma) \in \nabla_N \mathbb{T}(x; \lambda, \gamma). \quad (\text{A.2})$$

Then, by (A.2) and (2.1)-(2.3) the vector value function $F_1(\beta; d)$ is Newton differentiable and

$$\begin{bmatrix} H_{11}^k & H_{12}^k \end{bmatrix} \in \nabla_N F_1(z_{mcp}^k), \quad (\text{A.3})$$

where H_{11}^k, H_{12}^k are in the form of (2.17). By (2.1)-(2.3), $F_2(\beta; d)$ is Newton differentiable and

$$\begin{bmatrix} H_{21}^k & H_{22}^k \end{bmatrix} \in \nabla_N F_2(z_{mcp}^k), \quad (\text{A.4})$$

where H_{21}^k, H_{22}^k are in the form of (2.17). It follows (A.3)-(A.4) and (2.1)-(2.3) that $H_{mcp}^k \in \nabla_N F_{mcp}(z_{mcp}^k)$.

The uniform boundedness of $(H_{mcp}^k)^{-1}$ is derived similarly as the proof of Theorem 2.6 in [Yi and Huang (2017)].

APPENDIX E: Proof of Theorem 3.1

Proof: Here we give the proof for the results for MCP since the proof for SCAD penalty is similar. Let z_{mcp}^k be sufficiently close to z_{mcp}^* which is a root of F_{mcp} . By the definition of Newton derivative we have,

$$\|H_{mcp}^k(z_{mcp}^k - z_{mcp}^*) - F_{mcp}(z_{mcp}^k) + F_{mcp}(z_{mcp}^*)\|_2 \leq \varepsilon \|z_{mcp}^k - z_{mcp}^*\|_2, \quad (\text{A.5})$$

where $\varepsilon \rightarrow 0$ as $z_{mcp}^k \rightarrow z_{mcp}^*$. Then, by the definition of SSN and the fact $F_{mcp}(z_{mcp}^*) = 0$ we get

$$\begin{aligned} & \|z_{mcp}^{k+1} - z_{mcp}^*\|_2 \\ &= \|z_{mcp}^k - (H_{mcp}^k)^{-1}F_{mcp}(z_{mcp}^k) - z_{mcp}^*\|_2 \\ &= \|z_{mcp}^k - (H_{mcp}^k)^{-1}F_{mcp}(z_{mcp}^k) - z_{mcp}^* + (H_{mcp}^k)^{-1}F_{mcp}(z_{mcp}^*)\|_2 \\ &\leq \|(H_{mcp}^k)^{-1}\| \|H_{mcp}^k(z_{mcp}^k - z_{mcp}^*) - F_{mcp}(z_{mcp}^k) + F_{mcp}(z_{mcp}^*)\|_2 \\ &\leq M_\gamma \varepsilon \|z_{mcp}^k - z_{mcp}^*\|_2. \end{aligned}$$

The last inequality follows from (A.5) and the uniform boundedness of $(H_{mcp}^k)^{-1}$ proved in Theorem 2.2. Then the sequence z_{mcp}^k generated by Algorithm 2 converges to z_{mcp}^* locally superlinearly.

References

- Beck, A. and Teboulle, M. (2009). A fast iterative shrinkage-thresholding algorithm for linear inverse problems. *SIAM Journal on Imaging Sciences*, 2(1):183–202.
- Becker, S., Bobin, J., and Candès, E. J. (2011). NESTA: A fast and accurate first-order method for sparse recovery. *SIAM Journal on Imaging Sciences*, 4(1):1–39.

- Breheeny, P. (2017). Marginal false discovery rates for penalized regression models. *arXiv preprint arXiv:1607.05636v2*.
- Breheeny, P. and Huang, J. (2011). Coordinate descent algorithms for nonconvex penalized regression, with applications to biological feature selection. *The Annals of Applied Statistics*, 5(1):232.
- Breheeny, P. and Huang, J. (2015). Group descent algorithms for nonconvex penalized linear and logistic regression models with grouped predictors. *Statistics and Computing*, 25(2):173–187.
- Bühlmann, P., Kalisch, M., and Meier, L. (2014). High-dimensional statistics with a view toward applications in biology. *Annual Review of Statistics and Its Application*, 1:255–278.
- Buza, K. (2014). Feedback prediction for blogs. In *Data analysis, machine learning and knowledge discovery*, pages 145–152. Springer.
- Candes, E. J. and Tao, T. (2005). Decoding by linear programming. *IEEE Transactions on Information Theory*, 51(12):4203–4215.
- Chen, S. S., Donoho, D. L., and Saunders, M. A. (2001). Atomic decomposition by basis pursuit. *SIAM Review*, 43(1):129–159.
- Chen, X., Nashed, Z., and Qi, L. (2000). Smoothing methods and semismooth methods for nondifferentiable operator equations. *SIAM Journal on Numerical Analysis*, 38(4):1200–1216.
- Chen, X., Qi, L., and Sun, D. (1998). Global and superlinear convergence of the smoothing newton method and its application to general box constrained variational inequalities. *Mathematics of Computation of the American Mathematical Society*, 67(222):519–540.
- Donoho, D. L. and Johnstone, I. M. (1995). Adapting to unknown smoothness via wavelet shrinkage. *Journal of the American Statistical Association*, 90(432):1200–1224.
- Efron, B., Hastie, T., Johnstone, I., and Tibshirani, R. (2004). Least angle regression. *The Annals of Statistics*, 32(2):407–499.
- Fan, J. and Li, R. (2001). Variable selection via nonconcave penalized likelihood and its oracle properties. *Journal of the American Statistical Association*, 96(456):1348–1360.
- Friedman, J., Hastie, T., Höfling, H., and Tibshirani, R. (2007). Pathwise coordinate optimization. *The Annals of Applied Statistics*, 1(2):302–332.

- Friedman, J., Hastie, T., and Tibshirani, R. (2010). Regularization paths for generalized linear models via coordinate descent. *Journal of Statistical Software*, 33(1):1–22.
- Fu, W. J. (1998). Penalized regressions: the bridge versus the lasso. *Journal of Computational and Graphical Statistics*, 7(3):397–416.
- Huang, J., Breheny, P., Lee, S., Ma, S., and Zhang, C.-H. (2016). The mnet method for variable selection. *Statistica Sinica*, 26:903–923.
- Huang, J., Jiao, Y., Jin, B., Liu, J., Lu, X., and Yang, C. (2018). A unified primal dual active set algorithm for nonconvex sparse recovery. *arXiv preprint arXiv:1310.1147*.
- Huang, J., Jiao, Y., Lu, X., and Zhu, L. (2017). Robust decoding from 1-bit compressive sampling with least squares. *arXiv preprint arXiv:1711.01206*.
- Huang, J., Ma, S., and Zhang, C.-H. (2008). Adaptive lasso for sparse high-dimensional regression models. *Statistica Sinica*, 18:1603–1618.
- Ito, K. and Kunisch, K. (2008). *Lagrange multiplier approach to variational problems and applications*. SIAM.
- Jiao, Y., Jin, B., and Lu, X. (2015). A primal dual active set with continuation algorithm for the ℓ^0 -regularized optimization problem. *Applied and Computational Harmonic Analysis*, 39(3):400–426.
- Kummer, B. (1988). Newton’s method for non-differentiable functions. *Advances in mathematical optimization*, 45:114–125.
- Lange, K., Hunter, D. R., and Yang, I. (2000). Optimization transfer using surrogate objective functions (with discussion). *Journal of Computational and Graphical Statistics*, 9(1):1–59.
- Li, G. and Pong, T. K. (2017). Calculus of the exponent of kurdyka-lojasiewicz inequality and its applications to linear convergence of first-order methods. *Found Comput Math*, *In press*, <https://doi.org/10.1007/s10208-017-9366-8>.
- Li, X., Zhao, T., Yuan, X., and Liu, H. (2015). The flare package for high dimensional linear regression and precision matrix estimation in r. *Journal of Machine Learning Research*, 16(1):553–557.
- Mazumder, R., Friedman, J. H., and Hastie, T. (2011). Sparsenet: Coordinate descent with nonconvex penalties. *Journal of the American Statistical Association*, 106(495):1125–1138.

- Meinshausen, N. and Bühlmann, P. (2006). High-dimensional graphs and variable selection with the lasso. *The Annals of Statistics*, 34(3):1436–1462.
- Natarajan, B. K. (1995). Sparse approximate solutions to linear systems. *SIAM Journal on Computing*, 24(2):227–234.
- Osborne, M. R., Presnell, B., and Turlach, B. A. (2000). A new approach to variable selection in least squares problems. *IMA Journal of Numerical Analysis*, 20(3):389–403.
- Qi, L. and Sun, D. (1999). A survey of some nonsmooth equations and smoothing newton methods. In *Progress in optimization*, pages 121–146. Springer.
- Qi, L., Sun, D., and Zhou, G. (2000). A new look at smoothing newton methods for non-linear complementarity problems and box constrained variational inequalities. *Mathematical programming*, 87(1):1–35.
- Qi, L. and Sun, J. (1993). A nonsmooth version of newton’s method. *Mathematical programming*, 58(1-3):353–367.
- Scheetz, T. E., Kim, K.-Y. A., Swiderski, R. E., Philp, A. R., Braun, T. A., Knudtson, K. L., Dorrance, A. M., DiBona, G. F., Huang, J., Casavant, T. L., ShefiñAeld, V. C., and Stone, E. M. (2006). Regulation of gene expression in the mammalian eye and its relevance to eye disease. *Proceedings of the National Academy of Sciences of the United States of America*, 103(39):14429–14434.
- She, Y. (2009). Thresholding-based iterative selection procedures for model selection and shrinkage. *Electronic Journal of Statistics*, 3:384–415.
- Shi, Y., Jiao, Y., Cao, Y., and Liu, Y. (2018). An alternating direction method of multipliers for mcp-penalized regression with high-dimensional data. *Acta Mathematica Sinica, English Series*, <https://doi.org/10.1007/s10114-018-7096-8>.
- Tibshirani, R. (1996). Regression shrinkage and selection via the lasso. *Journal of the Royal Statistical Society. Series B (Methodological)*, 58(1):267–288.
- Tseng, P. (2001). Convergence of a block coordinate descent method for nondifferentiable minimization. *Journal of Optimization Theory and Applications*, 109(3):475–494.
- Wang, H., Li, B., and Leng, C. (2009). Shrinkage tuning parameter selection with a diverging number of parameters. *Journal of the Royal Statistical Society: Series B (Statistical Methodology)*, 71(3):671–683.

- Wang, H., Li, R., and Tsai, C.-L. (2007). Tuning parameter selectors for the smoothly clipped absolute deviation method. *Biometrika*, 94(3):553–568.
- Wang, L., Kim, Y., and Li, R. (2013). Calibrating nonconvex penalized regression in ultra-high dimension. *The Annals of Statistics*, 41(5):2505–2536.
- Wu, T. T. and Lange, K. (2008). Coordinate descent algorithms for lasso penalized regression. *The Annals of Applied Statistics*, 2(1):224–244.
- Yi, C. and Huang, J. (2017). Semismooth newton coordinate descent algorithm for elastic-net penalized huber loss regression and quantile regression. *Journal of Computational and Graphical Statistics*, 26(3):547–557.
- Zhang, C.-H. (2010a). Nearly unbiased variable selection under minimax concave penalty. *The Annals of Statistics*, 38(2):894–942.
- Zhang, C.-H. and Huang, J. (2008). The sparsity and bias of the lasso selection in high-dimensional linear regression. *The Annals of Statistics*, 36(4):1567–1594.
- Zhang, T. (2010b). Analysis of multi-stage convex relaxation for sparse regularization. *Journal of Machine Learning Research*, 11(Mar):1081–1107.
- Zhao, P. and Yu, B. (2006). On model selection consistency of lasso. *Journal of Machine Learning Research*, 7(Nov):2541–2563.
- Zou, H. (2006). The adaptive lasso and its oracle properties. *Journal of the American Statistical Association*, 101(476):1418–1429.
- Zou, H. and Li, R. (2008). One-step sparse estimates in nonconcave penalized likelihood models. *The Annals of statistics*, 36(4):1509–1533.

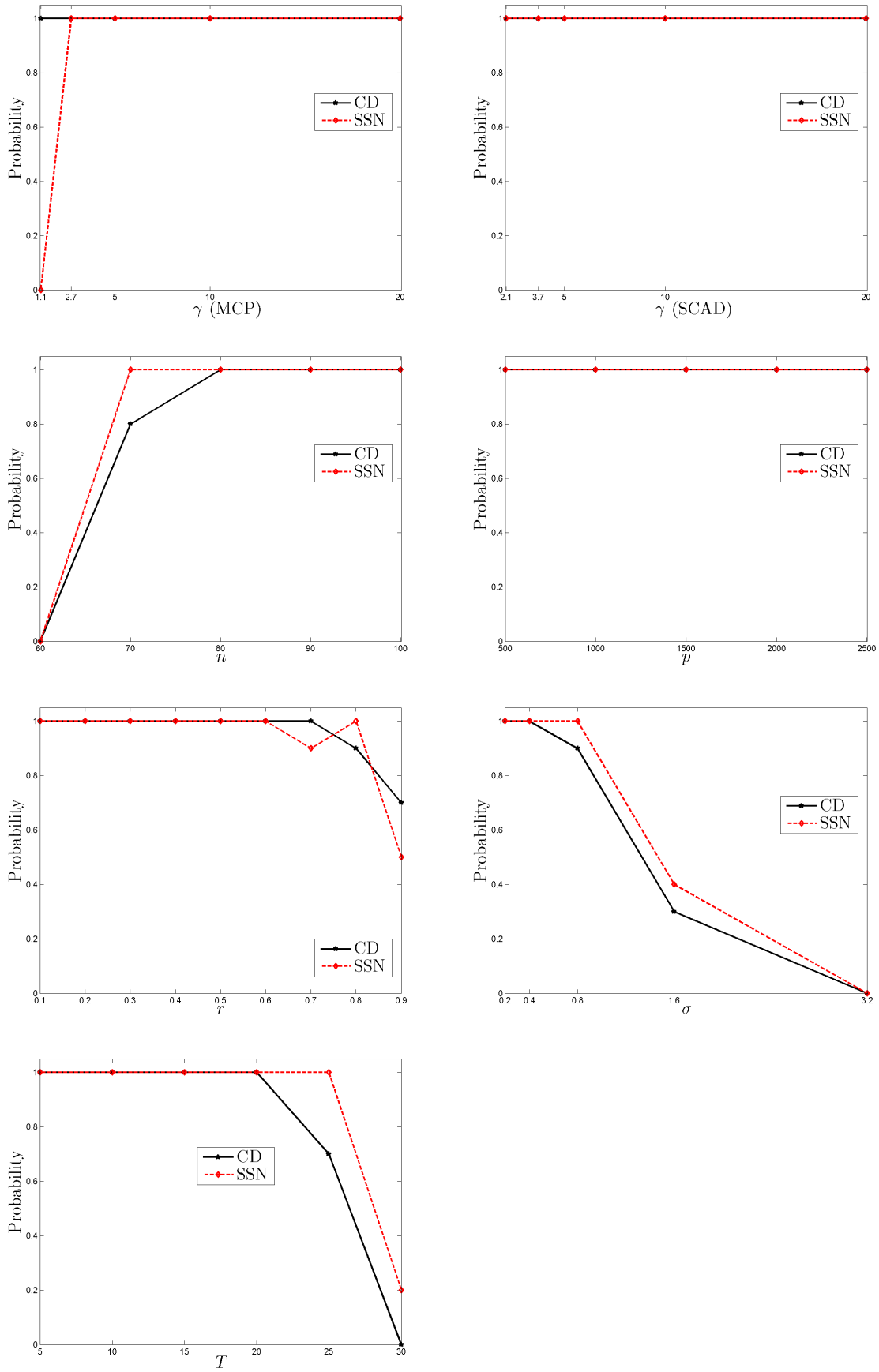


Figure 1: Numerical results of the influence of the model parameters on the exact support recovery probability.

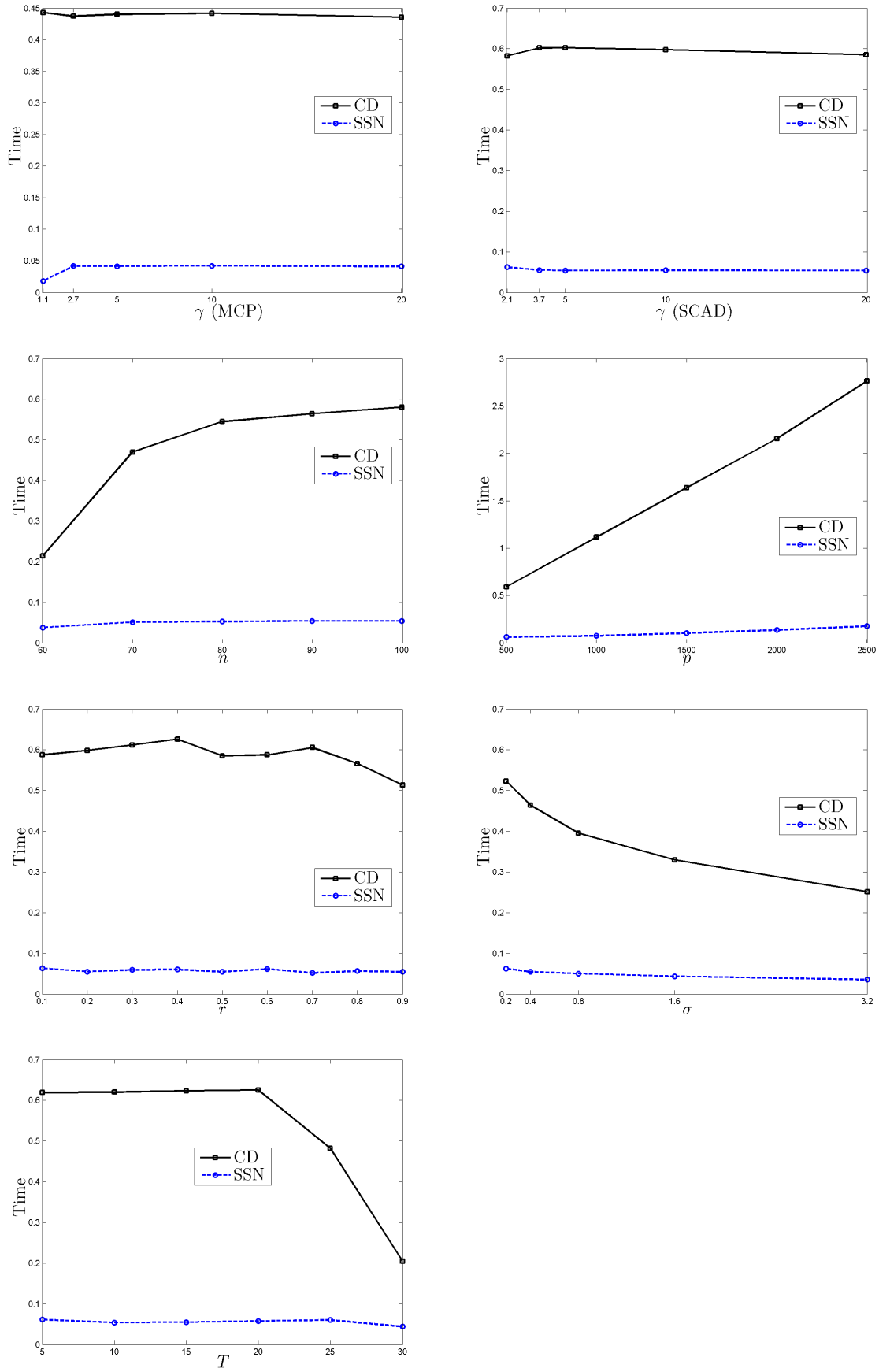


Figure 2: Numerical results of the influence of the model parameters on the CPU time.

Table 1: Simulation results with $n = \lfloor p/5 \rfloor$ and $T = \lfloor n/[2 \log(p)] \rfloor$ based on 100 independent runs.

p	r	σ	penalty	algorithm	Time	MS	CM	AE	RE
1000	0.3	0.1	MCP	CD	1.3458	14.00	100%	0.0142	0.0014
				SSN	0.1920	14.00	100%	0.0183	0.0018
		SCAD	CD	1.7671	14.00	100%	0.0150	0.0015	
			SSN	0.2068	14.00	100%	0.0188	0.0018	
		1	MCP	CD	0.8790	14.00	100%	0.1493	0.0147
				SSN	0.1228	14.00	100%	0.1504	0.0148
	SCAD	CD	1.1659	13.90	99%	0.1778	0.0174		
		SSN	0.1418	13.97	99%	0.1580	0.0152		
	0.5	0.1	MCP	CD	1.3387	14.00	100%	0.0153	0.0015
				SSN	0.1849	13.78	98%	0.1489	0.0132
		SCAD	CD	1.7413	14.00	100%	0.0148	0.0015	
			SSN	0.2238	14.00	100%	0.0187	0.0018	
		1	MCP	CD	0.8668	13.92	98%	0.1730	0.0171
				SSN	0.1309	13.92	98%	0.1735	0.0171
	SCAD	CD	1.1434	13.82	97%	0.1809	0.0191		
		SSN	0.1509	13.97	99%	0.1492	0.0147		
	0.7	0.1	MCP	CD	1.3677	14.00	100%	0.0149	0.0015
				SSN	0.1773	13.20	90%	0.3823	0.0434
		SCAD	CD	1.7679	14.00	100%	0.0146	0.0015	
			SSN	0.2168	14.00	100%	0.0190	0.0019	
		1	MCP	CD	0.8786	13.95	98%	0.1787	0.0169
				SSN	0.1175	12.35	76%	0.9406	0.0983
	SCAD	CD	1.1441	13.47	91%	0.4013	0.0424		
		SSN	0.1484	14.01	97%	0.1761	0.0166		
2000	0.3	0.1	MCP	CD	3.0636	26.00	100%	0.0113	0.0011
				SSN	0.7697	26.00	100%	0.0164	0.0015
		SCAD	CD	3.8884	26.00	100%	0.0119	0.0011	
			SSN	0.8128	26.00	100%	0.0169	0.0016	
		1	MCP	CD	2.0280	26.00	100%	0.1165	0.0108
				SSN	0.5568	26.00	100%	0.1169	0.0108
	SCAD	CD	2.5903	26.00	100%	0.1176	0.0109		
		SSN	0.5928	26.00	100%	0.1178	0.0109		
	0.5	0.1	MCP	CD	3.0998	26.00	100%	0.0122	0.0010
				SSN	0.6672	26.00	100%	0.0177	0.0015
		SCAD	CD	3.9453	26.00	100%	0.0117	0.0011	
			SSN	0.7062	26.00	100%	0.0168	0.0015	
		1	MCP	CD	2.0312	26.00	100%	0.1204	0.0104
				SSN	0.4682	26.00	100%	0.1206	0.0105
	SCAD	CD	2.6170	26.00	100%	0.1181	0.0105		
		SSN	0.5067	26.00	100%	0.1187	0.0105		
	0.7	0.1	MCP	CD	3.1308	26.00	100%	0.0121	0.0011
				SSN	0.6379	24.09	84%	0.6352	0.0607
		SCAD	CD	3.9982	26.00	100%	0.0117	0.0011	
			SSN	0.7078	26.00	100%	0.0178	0.0016	
		1	MCP	CD	2.0787	26.00	100%	0.1189	0.0107
				SSN	0.5186	24.59	82%	0.5718	0.0561
	SCAD	CD	2.6466	25.93	97%	0.1547	0.0134		
		SSN	0.5884	26.00	98%	0.1302	0.0115		

Table 2: Analysis of the eyedata set. Estimated coefficients of different methods are provided. The zero entries correspond to variables omitted.

No.	Term	Probe	flare	glmnet	ncvreg	MCP		SCAD	
						CD	SSN	CD	SSN
	Intercept		7.6975	7.7133	6.3610	5.7659	6.2905	7.1832	5.7829
1	β_{11}	6222	0.0130	0.0140	0	0	0	0	0
2	β_{42}	12085	0.0151	0.0140	0	0	0	0	0
3	β_{50}	14046	0	0	0	0	0	0.0005	0
4	β_{54}	14949	0.0147	0.0160	0	0	0	0.0038	0
5	β_{62}	15863	-0.0381	-0.0387	0	0	0	-0.0189	0
6	β_{71}	16984	0	0	0	0	0	-0.0052	0
7	β_{76}	17599	0	0	0	0	-0.0574	-0.0327	0
8	β_{87}	21092	-0.0933	-0.0932	-0.0642	0	0	-0.1033	0
9	β_{90}	21550	-0.0189	-0.0183	0	0	0	0	0
10	β_{102}	22140	0	-0.0027	0	0	0	0	0
11	β_{123}	23288	0	0	0	0	-0.0662	0	0
12	β_{127}	23804	-0.0074	-0.0078	0	0	0	0	0
13	β_{134}	24245	0.0169	0.0161	0	0	0	0	0
14	β_{136}	24353	-0.0260	-0.0275	0	0	0	0	0
15	β_{140}	24565	0.0144	0.0184	0	0	0	0	0
16	β_{146}	24892	0.0072	0.0079	0	0	0	0	0
17	β_{153}	25141	0.1472	0.1452	0.2702	0.3047	0.3423	0.2440	0.3020
18	β_{155}	25367	0.0093	0.0092	0	0	0	0	0
19	β_{180}	28680	0.0684	0.0687	0.1836	0.1953	0.2544	0.1868	0.1961
20	β_{185}	28967	-0.0829	-0.0845	-0.2655	-0.3108	-0.2659	-0.2313	-0.3116
21	β_{187}	29041	-0.0369	-0.0384	0	0	0	-0.0126	0
22	β_{188}	29045	-0.0068	-0.0073	0	0	0	0	0
23	β_{200}	30141	-0.0451	-0.0467	-0.0239	0	-0.1408	-0.0768	0
	Time		0.35	0.26	0.19	0.16	0.11	0.20	0.12
	PMSE		0.0048	0.0048	0.0051	0.0055	0.0049	0.0045	0.0055

Table 3: Analysis of the bcTCGA dataset. Estimated coefficients of different methods are provided. The zero entries correspond to variables omitted.

No.	Term	Gene	ALASSO	MCP		SCAD	
				CD	SSN	CD	SSN
	Intercept		-0.6786	-0.6722	-0.4223	-0.9269	-0.4552
1	β_{1743}	C17orf53	0.1208	0	0.2669	0.0979	0.3883
2	β_{2739}	CCDC56	0	0	0	0.0484	0
3	β_{2964}	CDC25C	0	0	0.1141	0.0360	0.0444
4	β_{2987}	CDC6	0	0	0	0.0089	0
5	β_{3105}	CENPK	0	0	0	0.0125	0
6	β_{4543}	DTL	0.2544	0.3978	0.1227	0.0886	0.0746
7	β_{6224}	GNL1	0	0	0	0	-0.1025
8	β_{7709}	KHDRBS1	0.1819	0	0	0	0
9	β_{7719}	KIAA0101	0	0	0	0	0.0675
10	β_{9230}	MFGE8	0	0	-0.1354	0	-0.0972
11	β_{9941}	NBR2	0.4496	0.4687	0.5581	0.2408	0.5319
12	β_{12146}	PSME3	0.1439	0	0	0.0746	0
13	β_{14296}	SPAG5	0.0035	0	0	0.0117	0.0688
14	β_{14397}	SPRY2	0	0	0	-0.0058	0
15	β_{15122}	TIMELESS	0	0	0	0.0322	0
16	β_{15535}	TOP2A	0	0	0	0.0299	0
17	β_{15882}	TUBA1B	0.0857	0	0.2675	0	0
18	β_{16315}	VPS25	0.2560	0.1974	0	0.0998	0
	Time		17.83	32.13	2.19	32.12	2.92
	PMSE		0.2116	0.2461	0.2105	0.2639	0.2117